Imaging of multi-well and multi-fiber walkaway DAS-VSP datasets in a CCUS demonstration project onshore Japan

Yuji Yamada, Shotaro Nakayama (INPEX Corporation), Takuji Mouri (Japan Organization for Metals and Energy Security), Manish Lal Khaitan, Philip Armstrong, Olga Podgornova (slb)*

Summary

Walkaway VSP data acquisition was carried out using distributed acoustic sensing (DAS) technology in a carbon capture utilization and storage (CCUS) demonstration project onshore Japan. The survey utilized multiple fibers permanently installed behind casing strings of two deviated wells. A complex pseudo-2D source geometry was applied due to logistical and operational constraints. This DAS-VSP survey aimed to obtain high-resolution borehole seismic images around the wells for detailed subsurface delineation and monitoring dynamic behaviors during CCUS operations.

The recorded datasets from different wells were jointly processed. Anisotropy estimation and correction were performed to enhance imaging quality. The applied migration algorithm facilitated the correction of fiber sensitivity, contributing to improved imaging results and revealing the detailed structural and stratigraphic features. The dataset also allowed for inelastic attenuation (Q) analysis, indicating high Q values with reliable confidence levels. The recorded datasets were also fed into elastic full waveform inversion (eFWI) to extract detailed subsurface properties. The inversion results yielded high-resolution compressional and share velocities (Vp and Vs).

Despite logistical challenges leading to limited source coverage, processing and analysis of multi-fiber and multi-well walkaway DAS-VSP data provided valuable insights into subsurface contexts, aligning reasonably well with borehole datasets. Overall, the CCUS project benefited from the acquired data, showcasing its potential for monitoring and understanding subsurface contexts in the targeted area.

Introduction

For a carbon capture utilization and storage (CCUS) project, two deviated wells, namely Well-1 and Well-2, were newly drilled in a depleted oil field onshore Japan. For monitoring purposes, a combination of surface seismic and borehole seismic datasets was acquired. The two wells are both equipped with permanently installed optical fibers (two fibers in Well-1 and one fiber in Well-2), and these three fibers were simultaneously utilized to record walkaway VSP data in both wells using distributed acoustic sensing (DAS) technology. The three fiber cables, used as receivers for DAS-VSP survey, were installed behind casing strings in each of these two wells.

Due to logistical limitations, such as large obstructions and strict regulations in the area, DAS-VSP survey employed a complex pseudo-2D source geometry, which was piecewise linear (Figure 1). A 43 second linear 6-80Hz sweep was applied using four vibrator units at each source point. Approximately 280 vibrator points were acquired in each well, with receivers spaced at 6.3 m and a gouge length of 17.55 m, covering a depth interval from the surface to the total depth of each well.

These multi-well and multi-fiber DAS-VSP datasets were jointly processed to obtain high resolution borehole seismic images in the vicinity of the wells. Additionally, eFWI was applied aiming at extraction of detailed subsurface properties such as Vp and Vs.

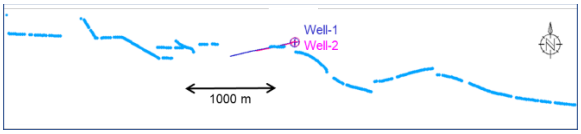

Figure 1: Source locations and well trajectories

Data QC and processing flow

Figure 2 shows the processing sequence applied to the DAS-VSP datasets. Overall, the quality of the data was variable well to well and varied within each well. The main source of noise was fiber ringing due to suboptimal coupling conditions. This was least apparent on a fiber installed behind the production casing of Well-1, and most apparent on a fiber installed behind the production casing of Well-2. Coupling related noise was strongest at the near offsets. For both wells, the signal-to-noise ratio (SNR) deteriorated rapidly with source offset and with increasing two-way-time.

Incoherent noise was mostly attenuated through shot domain low velocity noise modelling and removal in the tau-p domain and through median filtering and frequency-space domain filtering. Predictive deconvolution was applied to attenuate some fiber ringing and short-period multiples. Due to the low SNR at longer source offsets and the insensitivity of the fibers to broadside arrivals, time picking was possible only on a subset of the acquired data. These time picks were subsequently used for model calibration as well as for anisotropy estimation using phase slowness inversion. An initial 1D model was constructed using travel time tomography. The tomographic inversion was carried out first by estimating anisotropy parameters and then updating the P-wave velocity field. This 1D vertical transverse isotropy

(VTI) model was also used in conjunction with surface seismic common imaging point (CIP) tomography and structural information for joint inversion to build a more complex VTI model.

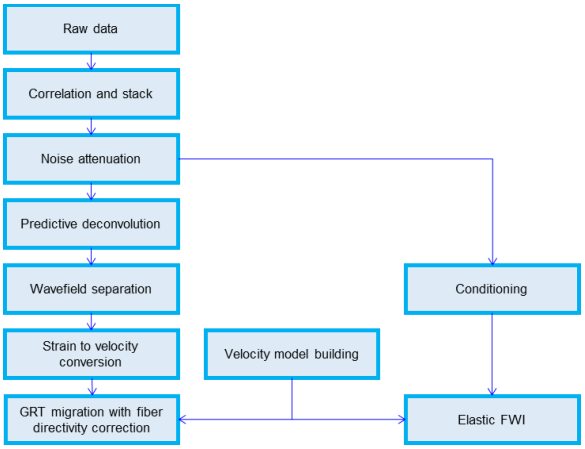

Figure 2: Processing sequence

DAS directivity correction (Sayed et. al., 2022) was also applied in the following two steps. First, data in the shot domain were scaled by the apparent velocity along the fiber length with a sparse linear Radon transform. This step transformed the measured fiber strain to velocity (assuming short gauge length compared to the wavelength of the P-wave events). The second correction, to address the directivity of the transformed velocity measurement, was performed during migration using anisotropic raytracing. Final imaging was done with ray-based generalized Radon transform (GRT) migration (Miller et. al. 1987), using both the simple 1D VTI model and a surface seismic velocity model calibrated with DAS-VSP datasets that also made use of the VTI parameters inverted from the VSP transit times.

To estimated detailed subsurface properties, data after the de-noising step were fed into eFWI (Podgornova, et al. 2022). Although the applied algorithm inverts for elastic properties including VTI parameters in a 2D sense, it can account for 3D acquisition effect, which can minimize irregularity in source geometry and well deviation out of the acquisition plane (Figure 1). The inverse scheme is formulated for DAS measurements, treated as averaged strain along wellbores over the applied gauge length, indicating that no data conversion was required in this case.

Imaging results

Initially, transit times picked on a near-offset shot gather were used to construct a vertical 1D compressional velocity profile. Travel time tomography was then used with a set of offset transit times to estimate VTI anisotropy. Phase slowness inversion (Miller et. al., 1994) was then applied to estimate VTI parameters in a more accurate manner. Based on fitting to a plot of vertical and horizontal slowness (Figures 3a and 3b), a Markov Chain Monte Carlo approach was used to estimate the likelihood of different parameter values (Figures 3c and 3d). Figure 3 shows the inversion results from two depth levels: one with strong anisotropy (Figures 3a and 3c) and the other one with weak anisotropy. In both cases, reasonable VTI estimates were attained, indicating the robustness of the approach. In our case, compressional velocity and Epsilon models were well constrained based on the information from surface seismic processing.

One advantage of the GRT migration algorithm is that it can store information on ray angles as well as ray propagation times. Therefore, the P-wave ray arrival angle at the receivers is available from the GRT migration. The dot product of a unit vector in this direction with a unit vector along the well axis gives the angle, θ, between the two vectors, which can then be used to derive a $1/\cos\theta$ correction term to compensate for the broadside insensitivity of the fiber. This directivity correction can then be applied as part of the migration process.

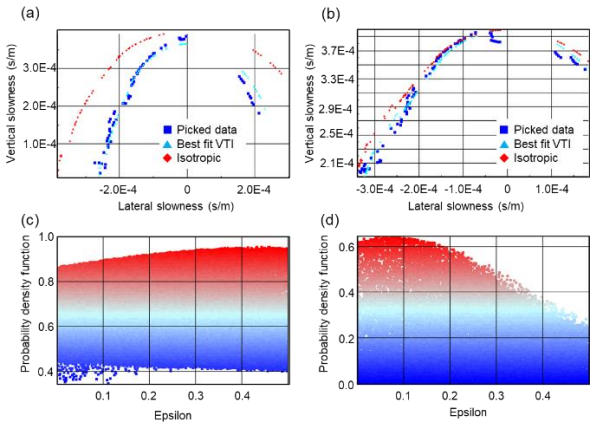

Figure 3: Phase slowness inversion results at two depth levels: (a) and (c) one depth level with strong anisotropy, and (b) and (d) one depth level with weak anisotropy. Plot colors in (c) and (d) signify values of probability density function ranging from 0.0 to 1.0.

Figure 4 shows migrated sections using data converted from strain to velocity in the preprocessing. The directivity correction was also applied. The dashed lines indicate well trajectories of Well-1 (cyan) and Well-2 (yellow). In Figure 4a, for this specific image, a dataset from Well-2 was used. Figure 4b shows a migrated section where datasets from three different fiber cables were jointly fed into a single imaging scheme. Despite the presence of quality difference among the datasets, the applied processing flow effectively minimize these effects. As a consequence, we collectively

utilized all the datasets. The combined imaging improved continuity of reflectors, extended imaging area, and enhanced well-seismic ties for two wells were confirmed.

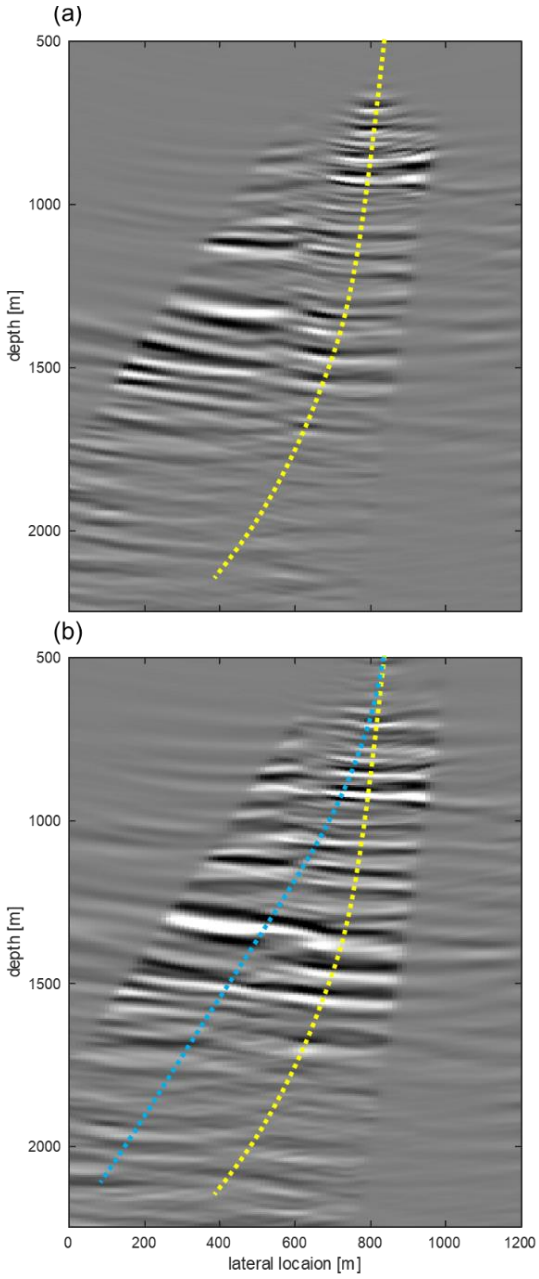

Figure 4: Migrated sections. (a) imaging result using data from Well-2 (its trajectory is indicated by a yellow dashed line), and (b) combined imaging result using data from two wells (its trajectory is indicated by a yellow and blue dashed lines).

In the migrated sections, minimal energy from reflectors extends beyond the west side of Well-1. The applied source and receiver geometries impose limitations, resulting in fewer ray paths from the west side arriving at the fibers in Well-1 and Well-2 compared to the east side. Nevertheless, it should be noted that our primary focus will be on the area between the two wells for monitoring dynamic behaviors during CCUS operations.

The zero-offset DAS-VSP data were also utilized for inelastic attenuation (Q) analysis. For this analysis, corrections for the gauge length effect and data conversion from strain to velocity were performed (Sayed et. al., 2021). There was almost minimal pulse broadening within the usable depth interval of the survey. Multi-spectral ratio analysis indicated Q values of around 200 or more. Figure 5 shows the results of the Q analysis. For the multi-spectral ratio, the results with relatively high confidence, as indicated by plots with warmer colors in Figure 5a, were obtained for large depth intervals where the midpoint is close to the center of the receiver array. In high Q formations, there is essentially no spectral change over small depth intervals, rendering Q analysis unreliable. For almost all cases, high Q values, i.e., greater than 150, employ high confidence. Examination of individual spectral ratios for depth intervals greater than 1000 m (Figure 5b) also indicates high Q values when considering spectral changes within the bandwidth of the applied sweep signature. High Q values generally provide little value in performing inverse-Q filtering, so we decided not to apply this process in our case.

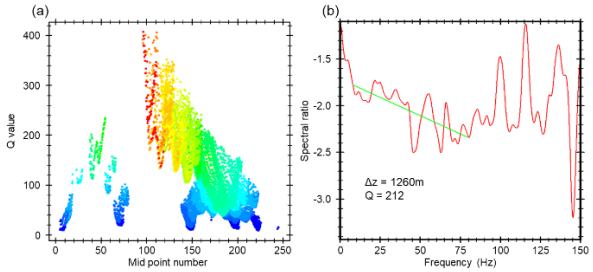

Figure 5: Q analysis: (a) multi-spectral ratio result, and (b) individual spectral ratio plot. Plot colors in (a) indicate confidence of Q analysis where warmer colors indicate higher confidence.

Elastic FWI

We further conducted eFWI that simultaneously inverted for Vp, Vs, density, and VTI anisotropy. Figure 6 shows the eFWI results that jointly utilized DAS data from Well-1 and Well-2. eFWI successfully resolved tilted layers around our target zone, i.e., the area between the two wells. Although depth imaging at deeper part was of lower quality due to weak P-wave reflections, velocity structures derived from eFWI provided clearer insights. Reasonable consistency

between the resultant velocity models and well logs was confirmed for both Well-1 and Well-2, indicating the robustness of the inversion results. Figure 7 shows a comparison between observed and synthetic data from eFWI, indicating the applied scheme reasonably explained both P and S wavefields and minimized misfit for data from both Well-1 and Well-2.

To mitigate adverse effect of complex acquisition geometry and data quality variation among datasets, we also conducted eFWI with different setups, such as the use of single well, shots from one side, sequential updates, etc. Although similar observations were made among different experiments, indicating stable inversion results, the combined utilization of these outcomes was of further help in interpretating subsurface properties and enabled us to assess its uncertainty.

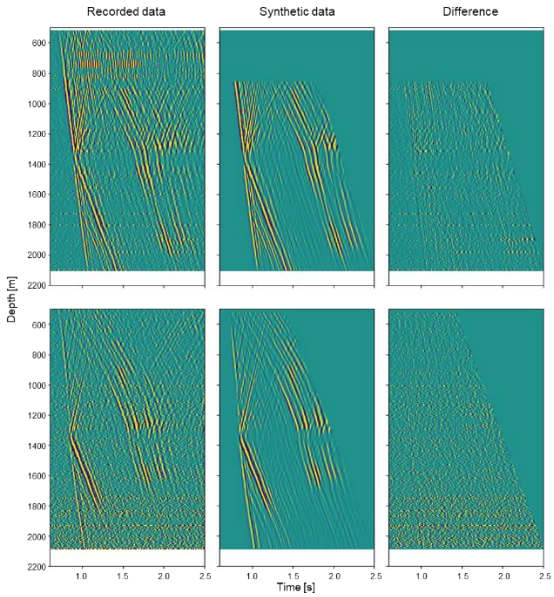

Figure 7 Comparison between recorded and synthetic data. Top and bottom figures are shot gathers from Well-1 and Well-2, respectively.

Conclusions

Although the acquisition of multi-well and multi-fiber walkaway DAS-VSP datasets faced logistical difficulties, leading to deficiencies in the recorded data, a considerable amount of beneficial information was obtained from the processed data. The depth imaging results attained sufficient coverage for the CCUS project by utilizing datasets from multiple wells. The outcomes yielded reasonable agreement with well data. To further extract detailed subsurface properties from DAS data, we applied eFWI. Despite the computational complexity and deficiency in the recorded data, due to its ability to account for both P-wave and S-wave energies, eFWI led to satisfactory outcomes and provided detailed insight into subsurface contexts.

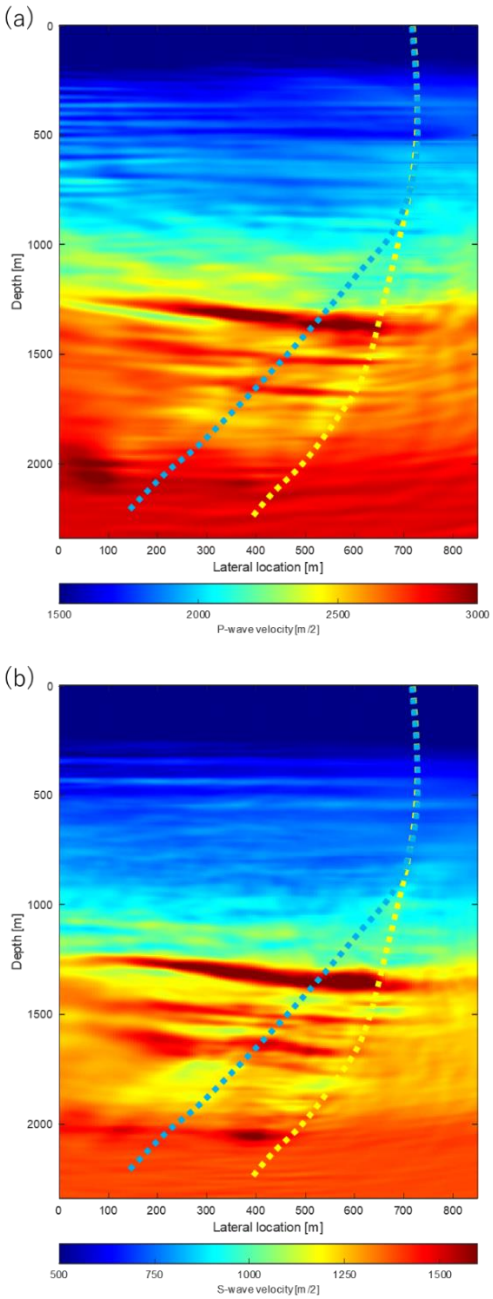

Figure 6: eFWI results. (a) P-wave velocity and (b) S-wave velocity. Dashed lines indicate well trajectories for Well-1 (cyan) and Well-2 (yellow).